Research Paper

Impact of Shear-Flexural Interaction on the Collapse Vulnerability of Tall Reinforced Concrete Frame-Wall Buildings

Mohammad Sadegh Barkhordari[1*] and Mohsen Tehranizadeh[2]

1. Ph.D., Department of Civil & Environmental Engineering, Amirkabir University of Technology (Tehran Polytechnic), Tehran, Iran,
*Corresponding Author; email: m.s.barkhordari@aut.ac.ir
2. Professor, Department of Civil & Environmental Engineering, Amirkabir University of Technology (Tehran Polytechnic), Tehran, Iran

Received: 16/05/2024
Revised: 10/06/2024
Accepted: 08/06/2024

ABSTRACT

Empirical studies have demonstrated a significant interaction between nonlinear flexural and shear responses in reinforced concrete shear walls. This paper investigates the implications of shear-flexural interaction (SFI) on the seismic performance of high-rise reinforced concrete dual frame-wall systems. Structures with three different heights (20, 25 and 30 stories) are analyzed. Comparative structural analyses are conducted using two modeling approaches for shear walls: one incorporating SFI and the other neglecting it. A set of ground motion records from the Federal Emergency Management Agency (FEMA) P695 is utilized to perform incremental dynamic analysis, facilitating a detailed evaluation of structural behavior under seismic loading. Collapse risk assessment encompasses seismic hazard analysis and the determination of collapse fragility. Furthermore, the collapse performance is appraised following the FEMA P695 methodology. The results underscore the substantial impact of SFI on both seismic performance and collapse risk in high-rise reinforced concrete structures. Specifically, integrating SFI into shear wall modeling results in elevated collapse risk and diminished ACMR. This underscores the pivotal role of SFI in shaping structural resilience.

Keywords:
Shear-flexure Interaction; Concrete shear walls; Seismic collapse analysis; FEMA P695; OpenSees

1. Introduction

Reinforced concrete (RC) shear walls are seismic lateral force resisting systems with extensive application in areas of high seismic hazard (Barkhordari et al., 2021). The role of RC shear walls is to provide deformation capacity and lateral strength during earthquake (Pizarro et al., 2023). Several studies have investigated RC shear wall structures under seismic excitement (Barkhordari & Tehranizadeh, 2020). Kim and Foutch (2007), assessed the seismic performance of the reinforced concrete shear wall buildings with three-, nine-, and twelve-stories using FEMA 355F techniques. The walls were simulated using uncoupled vertical flexural-springs and a horizontal shear-spring. Yang et al. (2012) evaluated the seismic performance characteristics of a tall reinforced concrete core wall building (a 42-story residential building) that was designed using two distinct design methodologies. The RC shear walls were simulated using uncoupled fiber-section model based elements and nonlinear shear springs. Beiraghi et al. (2015) used results of experimental testing of an 8-story RC shear wall to calibrate the fiber element model. Then, they evaluated the parameters of the damping, shear stiffness, axial load as well as longitudinal reinforcement ratio,

reporting that the moment and shear demand profile were sensitive to axial loading, and reinforcement ratio. Gogus and Wallace (2015) studied a variety of parameters of the seismic design categories using static pushover and incremental dynamic analysis for 20 special and 20 ordinary reinforced concrete walls. Sadraddin et al. (2016) studied the seismic responses of lower high-rise RC buildings (i.e. 10-story high to 20-story high) by considering different configurations of shear walls. A fiber method was employed to model the building members. Finally, fragility curves are derived for the three limit states using the results of incremental dynamic analysis. Nazari and Saatcioglu (2017) modeled four reinforced concrete shear wall buildings which had either a 2-story or a 5-story height in order to produce fragility curves corresponding to various performance levels. Shear walls were modeled using fiber-section model-based elements with uncoupled shear stress-shear strain relationship. They used the results of incremental dynamic analysis, finding that the life safety performance level of the 2010-building-designs was met. Dabaghi et al. (2019) modeled reinforced concrete shear wall buildings, with 4, 8, and 12 stories, subjected to ground motions, in order to evaluate changes in parameters such as the dimensions of the shear wall and boundary element, number of stories, and reinforcement detailing. They simulated shear walls using the shear-flexure element model to consider the shear-flexure interaction.

Shear walls are often divided into squat, moderate-aspect-ratio, and slender types based on their shear-span-to-depth ratio (Naderpour et al., 2022; Rezapour & Ghassemieh, 2023). Walls with their shear-span-to-depth ratio greater than 2.5-3 are referred to as slender walls (Gullu & Orakcal, 2021; Kolozvari et al., 2015). For decades, researchers assumed that the shear-flexural interaction (SFI) effects could be ignored in slender walls (Wu et al., 2017). Birely et al. (2011) carried out extensive experimental studies to determine the critical and effective parameters of wall responses. Results showed that the shear force has a considerable effect on wall behavior. Recent studies have shown that ignoring the SFI in RC walls-even those of the slender type-results in (1) overestimation of shear force demand in the plastic hinge region (Kolozvari & Wallace, 2016; Picon et al., 2023), (2) underestimation of shear deformations (Massone et al., 2009), (3) overestimation of lateral load capacity (Kolozvari, 2013), and (4) inaccurate calculation of flexural compression strains in the concrete (Kolozvari et al., 2019; Orakcal & Wallace, 2006). Kolozvari and Wallace (2016) have shown that using uncoupled models that consider predetermined nonlinear or linear behavior for shear force-deformation yield inaccurate results, in that the shear force demand of the wall is overestimated by almost 30%. On the other hand, the interstory drift is underestimated in the plastic hinge region by nearly 50% (Kolozvari et al., 2019). Pugh et al. (2017) used the FEMA P695 approach to determine the collapse risk of concrete shear wall buildings, which were designed based on current US codes. The wall heights changed from 6 to 30 stories. Under moderate to severe ground motion records, flexural over-strength of walls and inelastic response results in shear demands that are at least 2 to 4 times those calculated using an elastic design method. They concluded that there is a possibility for reduced flexural deformation capacity, which is attributable to shear-flexural interaction and shear-flexure failure.

Prior research has expanded our comprehension of RC shear wall dynamics (Barkhordari & Tehranizadeh, 2024; Massone et al., 2024; Soledispa et al., 2024; Tura et al., 2024), yet this body of work predominantly examines low to mid-rise structures and often employs specific modeling elements that overlook shear-flexural interaction (SFI). This study thus explores the influence of SFI on the dynamic behavior of concrete shear walls within high-rise buildings. We utilize an advanced nonlinear beam element (Barkhordari et al., 2021) incorporating a constitutive model derived from the Modified Compression Field Theory (MCFT), along with the DispBeamColumn element featuring uniaxial material properties. These elements are implemented within the OpenSees simulation software (FEMA, 2009; McKenna et al., 2009) to model the behavior of RC shear walls. This research primarily focuses on quantifying the structural collapse risk and assessing the collapse

performance using the FEMA P695 methodology (FEMA, 2009).

2. Method

The following sections provide a detailed description of the buildings, outline the design principles employed, and discuss the modeling assumptions made for the primary structural components.

2.1. Buildings Design

Shear wall-frame dual lateral resisting systems are adopted. The buildings had 20, 25 and 30 stories with a typical story height of 3.5 m. All buildings have identical floor plans with 30 × 30 m foot-prints and 6 m long spans (Figure 1). The design dead and live loads are, 5.5 kN/m^2 and 2.5 kN/m^2, respectively. The concrete compressive strength is assumed to be 55 MPa. Both longitudinal and transverse reinforcement have a yield strength of 420 MPa. The design was conducted based on ACI 318-14 (ACI, 2014) and ASCE 7-16 (ASCE, 2017). The building was designed based on the modal response spectrum analysis. The first 15 modes were used in the design. Table (1) presents the building site and the design parameters, where S_s and S_1 are the mapped maximum considered earthquake (MCE) spectral response acceleration parameter at short periods and 1-s period, respectively. The fundamental period of the buildings is presented in Table (2). The dimensional details of the beams, columns, and rebar sections of the concrete shear walls are presented in Appendix A.

Table 1. Buildings site and design parameters.

Latitude	Longitude	Design Category	Risk Category
35.6535	-120.4407	D	I
S_s (g) (MCE)	S_1 (g) (MCE)	Soil Classification	
1.5	0.6	D (Stiff Soil)	

Table 2. Fundamental period of buildings.

	20-Story	25-Story	30-Story
Modal Periods (s)	2.98	3.75	4.5

2.2. Analytical Modeling

Analytical models are generated in structural analysis software OpenSees (Mazzoni et al., 2006; McKenna et al., 2009). The concrete shear walls are modeled using two approaches. The first method (case 1), which is typical for macro simulation of slender walls, applies the beam-column element (DispBeamColumn), a methodology that was developed by Marafi et al. (2019). The DispBeamColumn is based on the displacement formulation. The primary assumption in its formulation is that the curvature is distributed linearly across the height of the element. This element incorporates Steel02 and Concrete02 uniaxial material (Mazzoni et al., 2006). The axial and flexural nonlinear response of RC walls are captured using DispBeamColumn (Marafi et al., 2019).

The second element is a Timoshenko beam-column (TimoBeamColumn), a methodology developed by Barkhordari et al. (2021) (case 2). The TimoBeamColumn uses the modified compression field theory (MCFT). The fiber-section Timoshenko element is free from shear-locking. Contrary to DispBeamColumn, TimoBeamColumn

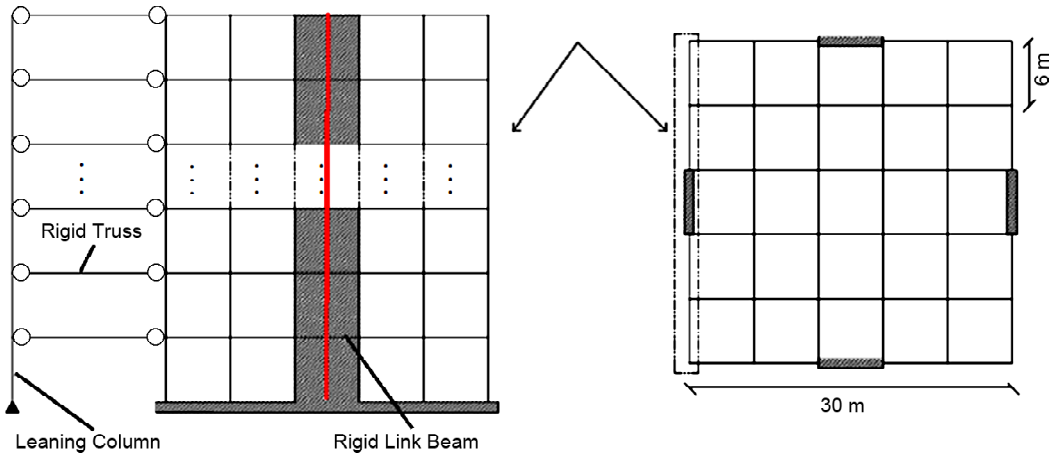

Figure 1. Typical plan and elevation views of the buildings.

captures interaction between axial/flexural and shear behavior of RC structural walls. The concrete crushing is expected to occur when concrete stress reaches zero in the descending branch of the Stress-strain relationship (Rashedi et al., 2022). Both elements use concrete stress-strain law that can consider the crushing of concrete.

In this study, the RC walls are modeled using three elements per story height. A two-dimensional model consisting of frame and wall (Figure 1) is used to simulate the building behavior. The torsional effects are ignored since the buildings are symmetric-plan and regular (DeBock et al., 2014). The gravity framing is considered using the leaning column, which is linked to the main structure (Figure 1). Rigid truss elements are used to link the shear wall-frame and leaning columns and transfer the P-Delta effect. Rayleigh damping is assumed. The nonlinear model uses the Rayleigh damping (2% critical damping ratio) for the analyses (Barkhordari et al., 2021).

The properties of the confined concrete are calculated using Mander et al.'s equations. Columns and beams are modeled using DispBeamColumn elements, Steel02 material, and Concrete02 material (Mazzoni et al., 2006). In Appendix B, the fundamental parameters for material properties have been listed.

2.3. Performance Assessment

The performance of the structures is investigated using FEMA P695 procedure (FEMA, 2009). This method uses the concept of scaling ground motion records in a way to cover the demand and capacity of a structure in a broad range from elastic behaviors to collapse (so-called incremental dynamic analysis (IDA)). The intensity of the records applied to the structure is represented by the intensity measure (IM), and the analysis outputs-or the structure's response-are shown with damage measure (DM). The first mode spectral acceleration Sa (T1, 5%) (FEMA, 2009) and the inter-story drift ratio (IDR) is selected as the IM and DM, respectively. The maximum IDR corresponding to the collapse limit is assumed to be 4% based on HAZUS (FEMA, 2003).

The 22 pairs of far-field ground motions of FEMA P695 are adopted for the IDA (FEMA, 2009). Detailed information about records can be found in FEMA P695. The characteristics of the selected ground motions are presented in FEMA P695. An IDA curve, which is a plot of IM versus DM, is obtained for each record.

The IDA curve is used to determine the collapse of the building (Pejovic & Jankovic, 2016). Fragility curves are generated using the log-normal cumulative dis- tribution function (Pejovic & Jankovic, 2016).

In this paper, collapse risk is also quantified using the seismic hazard at the site and the structure's collapse fragility curve. The method used by the United States geological survey (USGS) to create risk-targeted ground motion maps is utilized to compute collapse risk (Equations (1) and (2)).

$$\lambda_f = \int_0^{+\infty} \lambda_a f(a)\, da \tag{1}$$

$$P_{Co}^{50} = 1 - (1 - P(Collapse\ in\ 1\ year))^{50} \tag{2}$$

where λ_f is an annual rate of failure, λ_a is the mean annual frequency of IM exceedance, $f(a)$ is the probability density function of spectral acceleration and is the probability of collapse in 50 years.

3. Results and Discussion

The first step of the FEMA P695 (2009) methodology is to perform nonlinear static analysis to quantify the backbone curve of the structures. The analytical model is subjected to gravity analysis, followed by static pushover using the ASCE 7 (2017) load pattern. Figure (2) shows the pushover curves of the buildings. The ultimate displacement (δ_u), the effective yield roof drift displacement ($\delta_{y,eff}$) and the period-based ductility ($\mu_T = \delta_u / \delta_{y,eff}$) are presented in Table (3).

Table 3. Summary of the pushover analysis results.

Element	Structure	μ_T	δ_u (m)	$\delta_{y,eff}$ (m)
(Case 2) Timo.	20-Story	19	2.9	0.15
	25-Story	15.5	3.4	0.22
	30- Story	14	4	0.28
(Case 1) Disp.	20-Story	21	2.8	0.13
	25-Story	17.5	3.5	0.2
	30-Story	15.5	4.05	0.26

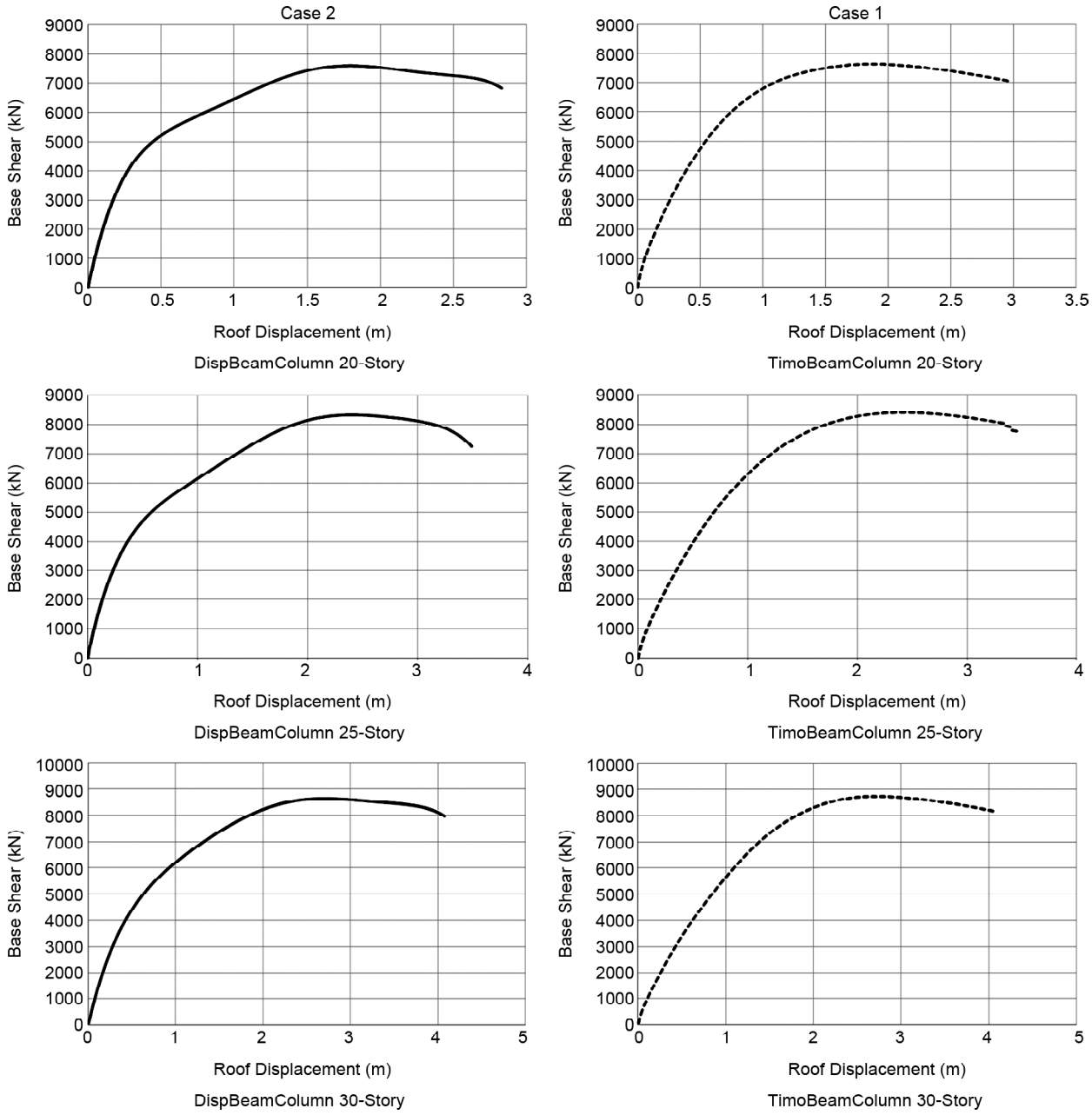

Figure 2. Pushover curves.

Based on the data presented in Figure (2) and Table (3), the pushover curves for the prototype buildings in case 2, where shear walls are represented using the TimoBeamColumn element, exhibit negligible differences compared to the pushover curves for case 1, where the shear walls are modeled using the DispBeamColumn element. The subsequent phase of the FEMA P695 methodology involves performing Incremental Dynamic Analysis (IDA) to derive collapse fragility curves from the obtained IDA results. Figures (3) and (4) illustrate the IDA curves and the resulting fragility curves for the buildings, respectively. Figure (4) indicates a clear trend: as the building height increases, the median collapse capacity demonstrates a decrease.

FEMA P695 (2009) utilizes a collapse margin ratio (CMR) to determine building seismic performance factor, which is defined as the ratio of the median spectral acceleration which causes collapse (S_{CT}) (Figure 4) to the MCE spectral acceleration (S_{MT}) at the first-mode period of the structure. The calculated CMR can be significantly affected by the spectral shape of a ground motion. Therefore, the adjusted collapse margin ratio (ACMR) is determined using the period-based

ductility (μ_T- Table 3) and a spectral shape factor (SSF- Table 4). The acceptable value of ACMR is obtained by considering the total system collapse uncertainty (Equation (3)) which is a function of the quality of test data (β_{TD}), record-to-record uncertainty (β_{RTR}), quality of design requirements (β_{DR}), and sophistication of modeling techniques (β_{MDL}).

Table 4. Results of FEMA P695 procedure.

Building	S_{MT}	S_{CT}	CMR	SSF	ACMR	Allowable ACMR	
						1.84	2.53
Case 2 20-St.	0.33	0.45	1.36	1.6	2.17	Pass	Ave. 2.35 Fail
Case 2 25-St.	0.27	0.39	1.44	1.6	2.3	Pass	
Case 2 30-St.	0.22	0.36	1.63	1.6	2.6	Pass	
Case 1 20-St.	0.33	0.61	1.84	1.6	2.9	Pass	Ave. 2.9 Pass
Case 1 25-St.	0.27	0.48	1.78	1.6	2.84	Pass	
Case 1 30-St.	0.22	0.42	1.9	1.6	3.04	Pass	

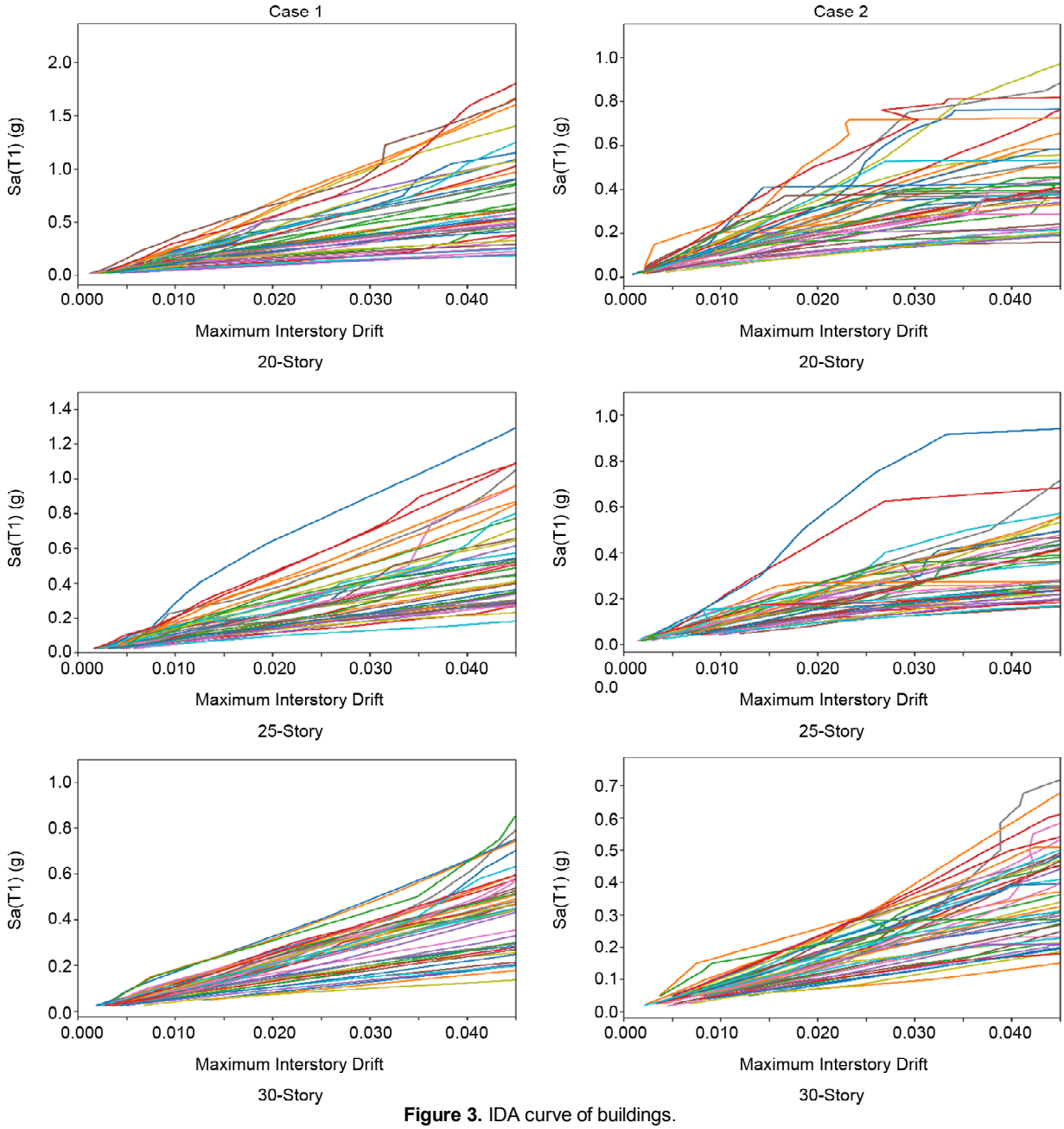

Figure 3. IDA curve of buildings.

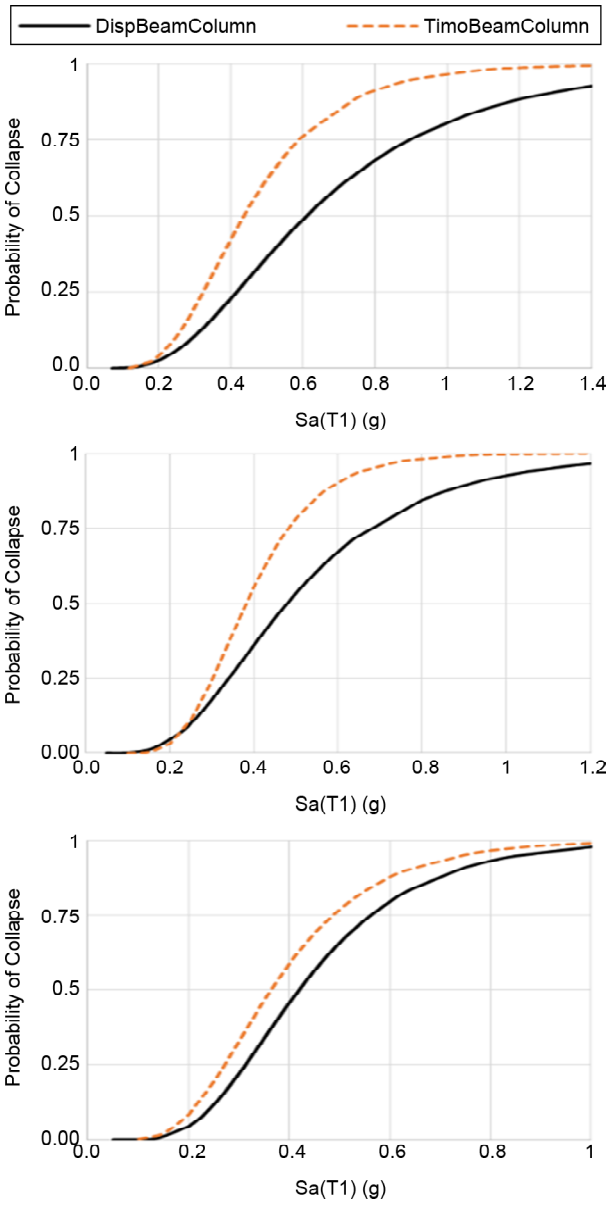

Figure 4. Fragility curve of buildings.

$$\beta_{TOT} = \sqrt{\beta_{RTR}^2 + \beta_{DR}^2 + \beta_{TD}^2 + \beta_{MDL}^2} \quad (3)$$

The buildings with μ_T value higher than or equal to 3.0 have a fixed β_{RTR} value of 0.40 (FEMA, 2009). For the other three uncertainty parameters, the following values are used, $\beta_{DR} = \beta_{TD} = \beta_{MDL} = 0.35$ by considering fair quality rating (FEMA, 2009). Hence, the acceptable values of the ACMR are obtained based on Table 7-3 of the FEMA P695 (2009), the values of 1.84 and 2.53 for $ACMR_{20\%}$ and $ACMR_{10\%}$, respectively. As summarized in Table (4), the ACMR values are lower for buildings whose shear wall is modeled using TimoBeamColumn element (case 2) than for buildings whose shear wall is modeled using DispBeamColumn element (case 1). For both cases, the ACMR of each prototype building is larger than the Acceptable $ACMR_{20\%}$. For case 1, the average ACMR across the performance group is greater than the acceptable value ($ACMR_{10\%} = 2.53$) but the buildings in case 2 fail to meet this performance requirement.

The collapse risk for the buildings is computed using Equations (1) and (2). Seismic hazard curves are obtained using the USGS unified hazard tool (USGS, 2020), as depicted in Figure (5). The hazard curve for a specific period is derived through interpolation. The computed collapse risks are summarized in Table (5). Table (5) reveals that, for case 2, where shear walls are modeled using the TimoBeamColumn element, the collapse risks are significantly higher compared to case 1, where shear walls are modeled using the DispBeamColumn

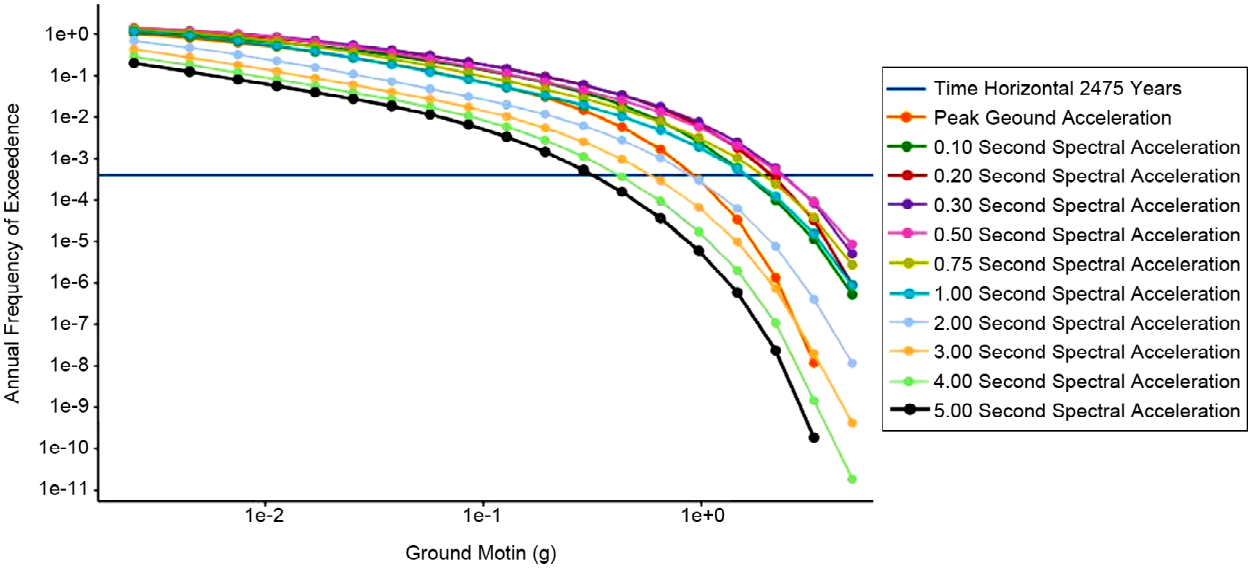

Figure 5. Seismic hazard curve.

Table 5. Collapse risk (%).

Type of Shear Wall Modeling	Number of Story		
	20	25	30
Case 2 (TimoBeamColumn Ele.)	5	3.94	3.17
Case 1 (DispBeamColumn Ele.)	2.15	2.35	1.7

element. Specifically, for case 2, buildings with 20, 25, and 30 stories exhibit collapse risks that are 2.32, 1.67, and 1.86 times greater than those in case 1, respectively. Additionally, no discernible trend is observed between the building height and collapse risk in case 1. To extend this analysis, it is essential to consider the implications of these findings on structural design and safety assessments. The higher collapse risk in case 2 suggests that the TimoBeamColumn element may capture certain nonlinear behaviors and failure mechanisms that the DispBeamColumn element does not, which could be critical for designing buildings in seismically active regions. Furthermore, the absence of a trend in collapse risk with increasing height for case 1 implies that other factors, such as the dynamic characteristics of the building and the interaction between different structural elements, might play a more significant role in determining collapse risk. These insights underscore the need for a nuanced approach to modeling and risk assessment that considers the complex interplay of various structural and seismic factors.

From the aforementioned review, several critical insights are evident:

- Increased ACMR with Building Height: As building height increases, the Adjusted Collapse Margin Ratio (ACMR) also increases (refer to Table 4). This trend aligns with the collapse risk values presented in Table (5), which show a decrease in collapse risk with increasing building height.
- Impact of Shear-Flexural Interaction on Collapse Risk: When shear-flexural interaction is accounted for in modeling the shear walls (case 2), buildings exhibit higher collapse risks and lower ACMR values. This observation is supported by prior research indicating that models that do not couple shear and flexural behaviors tend to underestimate inter-story drift at levels where wall yielding occurs (Barkhordari & Jawdhari, 2023). Consequently, these uncoupled models predict lower collapse risks and higher ACMR values (Kolozvari & Wallace, 2016; Safaeian Hamzehkolaei & Barkhordari, 2024).
- Comparison with ASCE 7 Performance Objectives: The calculated collapse risks exceed the ASCE 7 (2017) performance objective of a 1% probability of collapse over 50 years. The determination of an acceptable ACMR value involves subjective judgment (Zaker Esteghamati et al., 2018), particularly when considering the total system collapse uncertainty. Therefore, the direct method of calculating collapse risk and the FEMA P695 procedure, which incorporates the average ACMR across the performance group (Table 4), may yield differing performance predictions.

4. Conclusion

Recent experimental findings highlight the pronounced influence of shear-flexural interaction (SFI) on the global behavior of structural walls, even when flexural behavior predominantly governs design considerations. This study explored the implications of SFI on the performance of reinforced concrete (RC) dual high-rise buildings designed in accordance with contemporary building codes, focusing specifically on collapse behavior. To simulate the behavior of RC shear walls accurately, a sophisticated structural element was employed. This element captures the complex interplay between axial, flexural, and shear responses, in contrast to traditional fiber-type elements that overlook the SFI effect.

The research centered on dual systems, consisting of moment-resisting frames and RC shear walls, across 20, 25, and 30-story buildings. These structures were designed following the ACI 318-14 and ASCE 7-16 standards. Utilizing the advanced computational platform OpenSees, detailed analytical models of the buildings were developed. Two distinct modeling approaches were evaluated: Case 1 employed the DispBeamColumn element, while Case 2 utilized the TimoBeamColumn element. This comparison aimed to elucidate the impact of different modeling techniques on the structural response. The collapse performance was meticulously analyzed using the FEMA P695 procedure and

accompanying collapse risk assessments. The inclusion of SFI in the simulations of shear wall behavior revealed an increased collapse risk and a reduced average collapse margin ratio (ACMR). These findings underscore the significant variations in collapse risk calculations, advocating for the implementation of advanced modeling elements that effectively capture the nonlinear interaction between shear and flexure in RC shear walls. Therefore, integrating these sophisticated modeling techniques is recommended to improve the precision of structural evaluations and reduce potential collapse risks in high-rise buildings.

Future research should aim to refine and enhance the modeling techniques for shear-flexural interaction in RC shear walls. This includes the development of more advanced computational elements that can seamlessly integrate with existing structural analysis software. Additionally, experimental studies should be conducted to validate the accuracy of these models under various loading conditions and configurations. Investigating the effects of different material properties and construction methods on SFI is crucial for broadening the applicability of these models. Moreover, large-scale tests on physical models of high-rise buildings can provide invaluable data to further calibrate and validate computational models. Research should also explore the implementation of these advanced modeling techniques in the design and assessment of buildings in seismic-prone regions. Understanding how these models can be applied to retrofit existing structures to enhance their seismic resilience will be a key area of focus.

References

ACI. (2014). *Building Code Requirements for Structural Concrete (ACI 318-14) and Commentary (ACI 318R-14).*

ASCE. (2017). *Minimum Design Loads and Associated Criteria for Buildings and Other Structures.*

Barkhordari, M.S., & Tehranizadeh, M. (2020). Ranking passive seismic control systems by their effectiveness in reducing responses of high-rise buildings with concrete shear walls using multiple-Criteria decision making. *International Journal of Engineering*, *33*(8), 1479-1490.

Barkhordari, M.S., & Jawdhari, A. (2023). Machine learning based prediction model for plastic hinge length calculation of reinforced concrete structural walls. *Advances in Structural Engineering*, *26*(9), 1714-1734. https://doi.org/https://doi.org/10.1177/13694332231174252.

Barkhordari, M.S., & Tehranizadeh, M. (2024). Shear-flexural interaction effect on the collapse risk of high-rise reinforced concrete frame-wall structures. *9th International Conference on Seismology and Earthquake Engineering*, Iran.

Barkhordari, M.S., Tehranizadeh, M., & Scott, M. H. (2021). Numerical modelling strategy for predicting the response of reinforced concrete walls using Timoshenko theory. *Magazine of Concrete Research*, *73*(19), 988-1010.

Beiraghi, H., Kheyroddin, A., & Kafi, M. (2015). Nonlinear fiber element analysis of a reinforced concrete shear wall subjected to earthquake records. *Iranian Journal of Science and Technology Transactions of Civil Engineering*, *39*(C2+), 409-422.

Birely, A.C., Lowes, L.N., & Lehman, D.E. (2011). *Investigation of Performance of Slender RC Structural Walls*. NEESR-SG: Seismic Behavior, Analysis, and Design of Complex Wall Systems. University of Washington.

Dabaghi, M., Saad, G., & Allhassania, N. (2019). Seismic collapse fragility analysis of reinforced concrete shear wall buildings. *Earthquake Spectra*, *35*(1), 383-404.

DeBock, D.J., Liel, A.B., Haselton, C.B., Hooper, J.D., & Henige Jr, R.A. (2014). Importance of seismic design accidental torsion requirements for building collapse capacity. *Earthquake Engineering & Structural Dynamics*, *43*(6), 831-850.

FEMA. (2003). *HAZUS-MH MR4 Technical Manual. National Institute of Building Sciences and Federal Emergency Management Agency (NIBS and FEMA)*, 712.

FEMA. (2009). *Quantification of Building Seismic Performance Factors*. Washington, DC.

Gogus, A., & Wallace, J.W. (2015). Seismic safety evaluation of reinforced concrete walls through

FEMA P695 methodology. *Journal of Structural Engineering*, *141*(10), 04015002.

Gullu, M.F., & Orakcal, K. (2021). Nonlinear finite element modeling of reinforced concrete walls with varying aspect ratios. *Journal of Earthquake Engineering*, 25(10), 2033-2064. https://doi.org/https://doi.org/10.1080/13632469.2019.1614498

Kim, T., & Foutch, D.A. (2007). Application of FEMA methodology to RC shear wall buildings governed by flexure. *Engineering Structures*, *29*(10), 2514-2522.

Kolozvari, K. (2013). *Analytical Modeling of Cyclic Shear-Flexure Interaction in Reinforced Concrete Structural Walls* [UCLA].

Kolozvari, K., Biscombe, L., Dashti, F., Dhakal, R. P., Gogus, A., Gullu, M.F., Henry, R.S., Massone, L. M., Orakcal, K., & Rojas, F. (2019). State-of-the-art in nonlinear finite element modeling of isolated planar reinforced concrete walls. *Engineering Structures*, *194*, 46-65.

Kolozvari, K., Orakcal, K., & Wallace, J. (2015). *Shear-Flexure Interaction Modeling for Reinforced Concrete Structural Walls and Columns under Reversed Cyclic Loading*. Pacific Earthquake Engineering Research Center, PEER Report (12).

Kolozvari, K., & Wallace, J.W. (2016). Practical nonlinear modeling of reinforced concrete structural walls. *Journal of Structural Engineering*, *142*(12), G4016001.

Marafi, N.A., Ahmed, K.A., Lehman, D.E., & Lowes, L.N. (2019). Variability in seismic collapse probabilities of solid-and coupled-wall buildings. *Journal of Structural Engineering*, *145*(6), 04019047.

Massone, L.M., Letelier, C.N., Soto, C.F., Yanez, F.A., & Rojas, F.R. (2024). Experimental and analytical study of squat walls with alternative d etailing. *Computers and Concrete*, *33*(5), 497.

Massone, L.M., Orakcal, K., & Wallace, J.W. (2009). Modelling of squat structural walls controlled by shear. *ACI Structural Journal*, *106*(5).

Mazzoni, S., McKenna, F., Scott, M.H., & Fenves, G.L. (2006). OpenSees command language manual. *Pacific Earthquake Engineering Research (PEER) Center*, *264*.

McKenna, F., Scott, M.H., & Fenves, G.L. (2009). Nonlinear finite-element analysis software architecture using object composition. *Journal of Computing in Civil Engineering*, *24*(1), 95-107.

Naderpour, H., Sharei, M., Fakharian, P., & Heravi, M.A. (2022). Shear strength prediction of reinforced concrete shear wall using ANN, GMDH-NN and GEP. *Journal of Soft Computing in Civil Engineering*, *6*(1), 66-87.

Nazari, Y.R., & Saatcioglu, M. (2017). Seismic vulnerability assessment of concrete shear wall buildings through fragility analysis. *Journal of Building Engineering*, *12*, 202-209.

Orakcal, K., & Wallace, J.W. (2006). Flexural modeling of reinforced concrete walls-experimental verification. *ACI Materials Journal*, *103*(2), 196.

Pejovic, J., & Jankovic, S. (2016). Seismic fragility assessment for reinforced concrete high-rise buildings in Southern Euro-Mediterranean zone. *Bulletin of Earthquake Engineering*, *14*, 185-212.

Picon, C.P., Massone, L.M., & Lopez, C.N. (2023). A shear-flexure interaction model for column elements with biaxial loading. *Engineering Structures*, *293*, 116636. https://doi.org/https://doi.org/10.1016/j.engstruct.2023.116636.

Pizarro, P.N., Massone, L.M., & Rojas, F.R. (2023). Simplified shear wall building model for design optimization. *Journal of Building Engineering*, *76*, 107368. https://doi.org/https://doi.org/10.1016/j.jobe.2023.107368.

Pugh, J.S., Lowes, L.N., & Lehman, D.E. (2017). Accurate methods for elastic seismic demand analysis of reinforced concrete walled buildings. *Journal of Structural Engineering*, *143*(8), 04017062.

Rashedi, S.H., Rahai, A., & Tehrani, P. (2022). Seismic performance evaluation of RC bearing wall structures. *Computers and Concrete*, *30*(2), 113-126.

Rezapour, M., & Ghassemieh, M. (2023). Macroscopic modelling of the concrete shear wall with

asymmetrical openings. *Modares Civil Engineering Journal*, *23*(5), 0-0.

Sadraddin, H.L., Shao, X., & Hu, Y. (2016). Fragility assessment of high-rise reinforced concrete buildings considering the effects of shear wall contributions. *The Structural Design of Tall and Special Buildings*, *25*(18), 1089-1102.

Safaeian Hamzehkolaei, N., & Barkhordari, M.S. (2024). Efficient ensemble learning-based models for plastic hinge length prediction of reinforced concrete shear walls. *Journal of Soft Computing in Civil Engineering*, *8*(3).

Soledispa, C.E., Pizarro, P.N., & Massone, L.M. (2024). Optimizing reinforced concrete walls and columns through artificial neural networks with structural neighbor-based features. *Journal of Building Engineering*, *89*, 109223. https://doi.org/10.1016/j.jobe.2024.109223.

Tura, C., Aydin, S., Yazgan, U., Orakçal, K., Ilki, A., Kabeyasawa, T., & Kang, J.-D. (2024). Critical issues in nonlinear modeling of reinforced concrete buildings: Code-compliant modeling approaches and the 2015 E-defense shake table tests on a full-scale 10-story building. *Bulletin of Earthquake Engineering*, *22*(2), 329-364. https://doi.org/10.1007/s10518-023-01772-1.

USGS. (2020). Unified hazard tool. Vailable at: https://earthquake.usgs.gov/hazards/interactive/.

Wu, Y.-T., Lan, T.-Q., Xiao, Y., & Yang, Y.-B. (2017). Macro-modeling of reinforced concrete structural walls: State-of-the-Art. *Journal of Earthquake Engineering*, *21*(4), 652-678.

Yang, T., Moehle, J., Bozorgnia, Y., Zareian, F., & Wallace, J. (2012). Performance assessment of tall concrete core-wall building designed using two alternative approaches. *Earthquake Engineering & Structural Dynamics*, *41*(11), 1515-1531.

Zaker Esteghamati, M., Banazadeh, M., & Huang, Q. (2018). The effect of design drift limit on the seismic performance of RC dual high-rise buildings. *The Structural Design of Tall and Special Buildings*, *27*(8), e1464.

Appendix A

Table A.1. Shear wall section of the prototype buildings.

Building	No. of Story	Thickness (cm)	Longitudinal Rein.	Transverse Rein. (cm^2/m)
10-Story	1-4	35	#6@20cm	8.8
	5-8	30	#5@20cm	7.5
	9-10	25	#4@20cm	6.3
15-Story	1-5	30	#5@20cm	7.5
	6-10	30	#4@25cm	6.3
	11-15	25	#4@25cm	6.3
20-Story	1-5	35	#6@20cm	8.8
	6-10	30	#5@20cm	7.5
	11-15	25	#4@20cm	6.3
	16-20	25	#4@25cm	6.3
25-Story	1-5	35	#6@15cm	8.8
	6-10	30	#6@20cm	7.5
	11-15	30	#5@20cm	7.5
	16-20	30	#4@20cm	7.5
	21-25	25	#4@25cm	6.3
30-Story	1-5	35	#7@20cm	8.8
	6-10	35	#6@20cm	8.8
	11-15	30	#5@20cm	7.5
	16-20	30	#5@25cm	7.5
	21-25	25	#4@20cm	6.3
	26-30	25	#4@25cm	6.3

Appendix B

Table B.1. Parameters of Steel02 material.

Yield Strength	Initial Elastic Tangent	Strain-Hardening Ratio
420 MPA	200 GPa	0.01

Table B.2. Parameters of MCFT material.

Concrete Compressive Strength (MPa)		Concrete Strain at Crushing Strength		Concrete Modulus of Elasticity	Tensile Strength
Unconf.	Confined	Unconf.	Confined	37 GPa	1.9 MPa
55	66	-0.005	-0.008		

Table B.3. Parameters of Concrete02 material.

Concrete Compressive Strength (MPa)	Unconf.	55
	Confined	66
Concrete Strain at Crushing Strength	Unconf.	-0.005
	Confined	-0.008
Concrete Crushing Strength (MPa)	10.0	
Concrete Strain at Maximum Strength	-0.002	
Ratio between Unloading Slope	0.15	
Tensile Strength	1.9 (MPa)	
Concrete Modulus of Elasticity	37 GPa	